ISBN-978-989-9121-29-4
ISTANBUL 25th International Conference on "Innovations in Engineering, Technology & Health Sciences" (IIETH-23)
Sept. 5-7, 2023 Istanbul (Turkiye)

On the Use of Contactless Vibration to Improve the Welding Quality

[1]Mohamad Salimi, [1]Ahmed Teyeb, [1]Evelyne El Masri, [2]Samiul Hoque, [2]Phil Carr,
[1]Wamadeva Balachandran[1], [1,3]Tat-Hean Gan

[1] Brunel University London, Uxbridge UB8 3PH, UK
[2] Carr's Welding Technologies Ltd. (CWT), Kettering, NN16 8PX, UK
[3] TWI Ltd., Granta Park, Great Abignton, Cambridge, CB 21 6AL, UK
ahmed.teyeb@brunel.ac.uk(A.T.); tat-hean.gan@brunel.ac.uk

Abstract: *This paper investigates the use of contactless power ultrasonic excitation to decrease the electrical impedance of the weld in laser welding. The literature extensively documents the impact of employing contact power ultrasonic excitation on the microstructure morphology and refinement of grain in the weld. This study involves characterising an industrial High Power Ultrasound Transducer (HPUT) by determining the optimal distance and angle for contactless excitation of the fusion zone in the weld, aiming to achieve the maximum amplitude. Subsequently, the transducer is integrated into the laser welding system, resulting in the creation of an ultra-sonic-assisted welding system. To find the improvement due to the contactless vibration assistance, the welding area was characterised by an impedance ohmmeter device. The results indicate an approximately 6 % improvement in the welding quality in terms of the impedance value, an important parameter for battery pack welding. In response to the issue of overheating in the industrial transducer during prolonged welding operations, an alternative transducer was proposed to overcome this challenge. Further investigations are carried out by the alternative transducer to find the effect of different wave types, namely, shear and compressional waves, on the welding quality. The contact vibration can excite the plate approximately 50 times higher in acceleration amplitude than contactless excitation. Nevertheless, enhancements of 10% and 6% are observed in the impedance value when utilising compressional and shear waves, respectively, as compared to the results obtained with contactless vibration.*

Keywords: *Low intensity ultrasound vibration, ultrasonic assistance welding, high power ultrasound transducer*

1. Introduction

Nowadays, several manufacturing processes such as laser welding, additive manufacturing and casting are based on the total fusion of material, followed by rapid solidification [1–3]. The material's structure in the final phase and its mechanical and electrical properties strongly depend on the solidification phase [4–6]. This phenomenon becomes particularly apparent when the material comprises a metal alloy or a combination of two different materials. For instance, when specific connectors are joined to battery cells through lap joining, typically using laser welding, during the production of battery packs for electric vehicles. [7,8]. The assembly of battery packs powering EVs is a hot topic that attracts the attention of researchers and industrials. The integrity of the assembly plays a crucial role in the reliability of the battery pack as well as in its electrical performance [9,10].

The variation in melting temperatures among different metals results in the simultaneous presence of liquid and solid phases. This means that particles with similar characteristics tend to cluster together within the molten pool [11,12], which ideally should be dispersed homogeneously throughout the liquid phase during solidification [13]. The occurrence of voids and gas, along with the variability in grain size, are commonly observed phenomena. These phenomena can lead to a degradation of the final material's properties [14,15], leading to problems such as hot cracking [16]. Therefore, the battery connection might be fragile and exhibit significant electrical resistance, resulting in energy wastage and increased battery pack temperatures. [17,18].

Ultrasonic-assisted laser welding is a welding technique where ultrasonic vibrations and laser energy are applied simultaneously. The ultrasonic vibrations, usually ranging from 20 to 40 kHz, generate controlled mechanical oscillations at the welding interface. These vibrations yield positive outcomes such as better material flow, improved diffusion, and increased malleability [19–21]. Conversely, the laser energy supplies localised heat to melt and fuse the materials together [22–24]. By incorporating ultrasonic vibrations alongside the welding, the integration facilitates superior blending of materials, resulting in robust and dependable welds. This combination effectively addresses concerns such as porosity, insufficient fusion, and cracking, thereby elevating the overall quality and integrity of the welds [25–27].

Typically, vibration-assisted welding utilises High Power Ultrasonic Transducers (HPUTs) to induce out-of-plane displacement using contact excitation. The main focus of this research revolves around utilising contactless vibration to enhance the quality of spot welding. For this purpose, a detailed characterisation of an ultrasound transducer equipped with a focused horn, capable of integration with a laser welding system, was conducted. The characterisation involved determining the optimal angle and distance for generating maximum vibration. The results obtained from both non-ultrasound welding and contactless vibration-assisted welding were analysed. The data indicated a decrease in welding impedance value of the weld when contactless vibration was employed. Furthermore, this study examines the impact of employing contact vibration, specifically generating mainly shear or compressional waves, to evaluate its effects on the welding impedance value. To connect the battery cell through ultrasonic-assisted laser welding, most clients prefer to have low-intensity vibration on their battery cells to prevent the generation of shock waves which can damage the key parts in a battery. Therefore, this study compares the outcomes of contact vibration with contactless vibration-assisted welding and non-ultrasonic welding to provide a comprehensive analysis of their respective results.

2. Contactless Vibration of the Plate

This section focuses on the characterisation of an industrial High-Power Ultrasonic Transducer (HPUT) named Q55, aiming to determine the optimal output of contactless vibration from this device. The transducer is comprised of a long-focused horn, which is conveniently connected to the transducer itself through a user-friendly amplifier (see Fig. 1). The Q55 is an ultrasonic processor that offers a compact and affordable solution, taking up minimal bench space. It is particularly suitable for standard cell disruption and various small volume applications. The transducer associated with this model has a power rating of 55 watts, operates at a frequency of 20 kHz, and has dimensions of 203mm × 190mm × 146mm (width × length × height). The accompanying horn for this transducer features a tip diameter of 2mm and a maximum displacement of 200 μm [28].

(**a**) (**b**)

Fig. 1. (a) The Q55 transducer with the needle horn that can be screwed into the transducer, (b) the power amplifier.

In this study, the objective is to weld two L-shaped plates together. To achieve this, it is beneficial to position the HPUT at an angle that can generate the highest vibration amplitude on the plate. By doing so, the maximum vibration amplitude can be transmitted to the molten pool area, enhancing the welding quality. To characterise the transducer, the vibration it generates is applied to an L-shaped plate at various angles ranging from 5 degrees to 80 degrees. This range of angles allows for a comprehensive assessment of the transducer's performance and its impact on the plate's response. The plate was made of aluminum alloy 1050 and has a thickness of 2 mm. To measure the response of the plate, a 3D laser vibrometer is employed, as depicted in Fig. 2. The plate's response is collected in three perpendicular directions: 1) the out-of-plane displacement along the z-direction, 2) the in-plane vibration along the x-direction, and 3) the in-plane vibration along the y-direction. While the L plate remains fixed and firmly attached to its base, the position of the transducer can be adjusted accordingly.

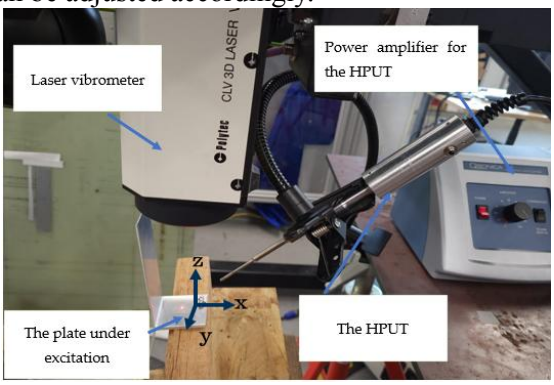

Fig. 2. The plate configuration, made of aluminium alloy 1050, for vibration measurement in the three orthogonal directions.

The out-of-plane vibration of the plate (the z-axis) is illustrated in Fig. 3. The maximum vibration level from the plate was recorded at 60 degrees and the minimum at 5 degrees. The observed amplification of vibration at a 60-degree angle could potentially be attributed to the reflection of contactless vibration from the first plate to the second plate. This reflection results in a higher overall vibration compared to the 80-degree angle configuration. Some of the additional frequency components present in the output signal apart from the fundamental frequency are referred to as harmonics which are integer multiples of the fundamental frequency. The rest arise due to factors such as non-linearities, mechanical resonances, and impedance mismatches.

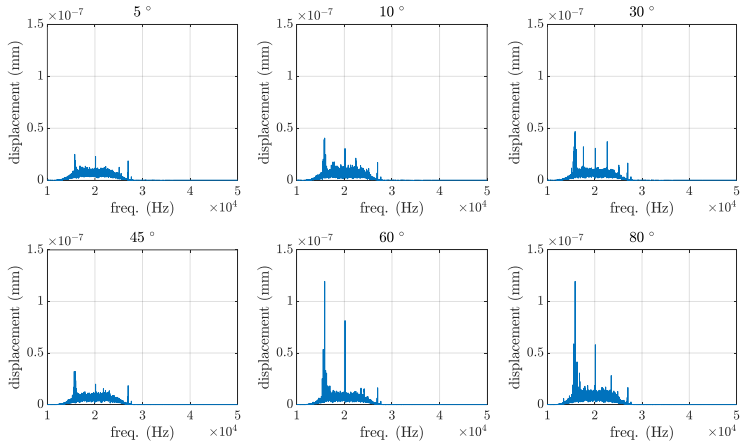

Fig. 3. The plate vibration in the vertical direction, the z-axis, increases the transducer angle from approximately 5^0 to 80^0.

The plate response under the contactless excitation for the x-axis, parallel to the direction of excitation, is plotted in Fig. 4. The maximum vibration level from the plate was recorded at 60 degrees and the minimum at 5 degrees. Similar to the previous findings, the maximum level of vibration occurs at a 60-

degree angle. This phenomenon is likely attributed to the reflection of vibrations from the first plate to the second plate, leading to an increased overall in-plane vibration compared to the configuration with a 5-degree angle.

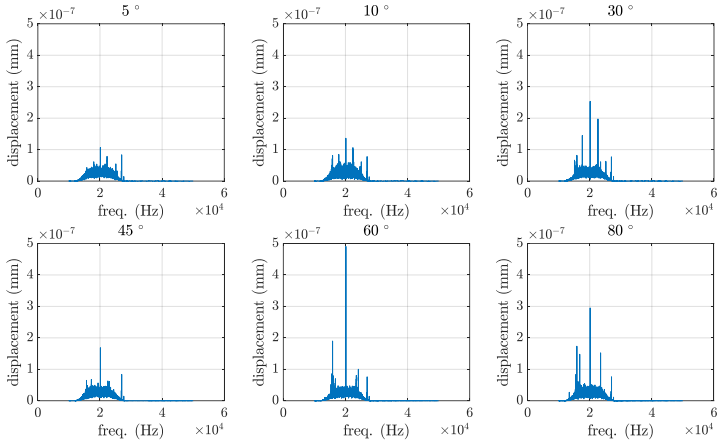

Fig. 4. The plate vibration in the horizontal direction, the x-axis, increases the transducer angle from approximately 5 ^{0} to 80 ^{0} .

In-plane vibration of the plate in the perpendicular direction to the direction of excitation, the y-axis, is plotted in Fig. 5. As in the previous directions, the highest level of vibration occurs at a 60-degree angle. This could be attributed to the reflection of vibrations from the first plate to the second plate, resulting in an increased overall in-plane vibration compared to the configuration with a 5-degree angle.

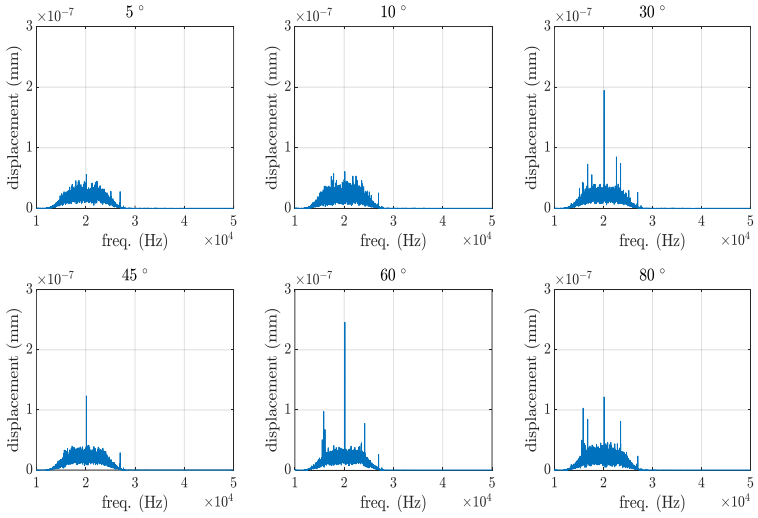

Fig. 5. The plate vibration in the horizontal direction, the y-axis, by increasing the transducer angle from approximately 5 ^{0} to 80 ^{0} .

In addition, this study aimed to determine the optimal distance between the tip of the transducer horn and the desired structure, which would result in the highest contactless vibration. To assess this, the effect of varying distances between the two was measured, and the results are presented in Fig. 6. It was found that the vibration level reached its peak when the gap between the structure and the tip of the transducer horn was 20 mm. Subsequently, as the gap increased to 25 mm, the vibration amplitude decreased by half. These findings highlight the importance of the distance between the transducer and the structure in achieving the desired vibration levels.

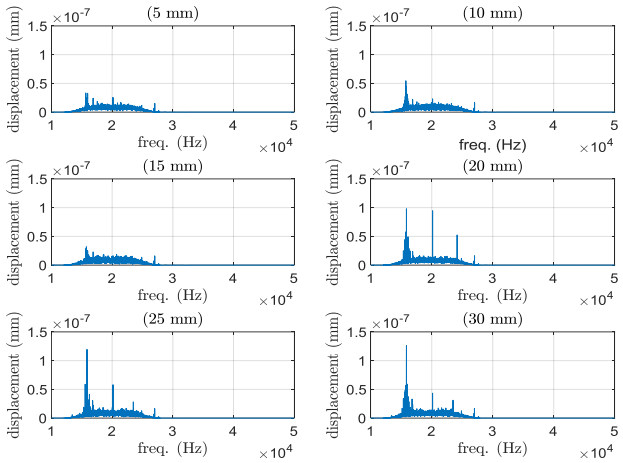

Fig. 6. The effect of the distance between the tip of the transducer horn and the structure on the contactless vibration specifically in the vertical direction, referred to as the z-axis.

Depending on the length of the gap, there will be resonance or standing wave field. For this case, the wavelength, λ, in the dry air can be estimated by $\lambda = c/f$, where c is the wave speed (343 m/s) and f is the frequency (20 kHz). Resonance occurs at every $(2n-1)\lambda/4$ distance, where n is an integer number. Consequently, the distances of 4.3 mm, 12.9 mm, 21.5 mm, and so on are expected to yield the highest vibration amplitudes. These distances correspond to the intervals determined by the resonance condition mentioned earlier, where the vibration amplitudes are likely to be maximised.

3. Impedance Testing

To measure the electrical resistance of lap joints that simulate EV battery connections, the Seaward Cropico DO7 Portable Digital Micro Ohmmeter is used. This measurement aims to find the effect of contactless vibration on reducing the welding resistance compared with non-ultrasound samples.

The Digital Micro Ohmmeter can be used for measuring very low electrical resistances in various applications, including the testing of various applications, including electrical connectors, switches, and fuses. It is commonly used in the automotive, aerospace, and energy sectors, where high accuracy and precision are critical.

The DO7 micro-ohmmeter, illustrated in Fig. 7, operates by passing a small electrical current through the two bottom ends of the welded plate followed by measuring the voltage drop at an area close to the weld. The resistance is then calculated using Ohm's Law (R = V/I), where R is resistance, V is voltage, and I is current. The instrument is designed to provide accurate readings of resistances ranging from less than 1 micro-ohm to 60 ohms, with a resolution of 0.1 micro-ohms.

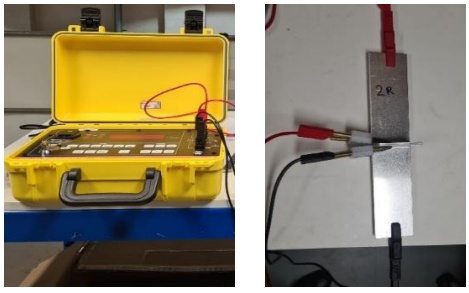

(**a**) (**b**)

Fig. 7. The welding is applied in the middle of two L-shaped plates and the impedance analysis is applied to two sides of the welded plate. (a) the Seaward Cropico DO7 Portable Digital Micro Ohmmeter and (b) the welded plate under investigation.

4. Ultrasonic assistance welding

Although contactless excitation is this paper's ultimate aim, it is worth checking the effect of other remote vibrations that can generate mainly shear and compressional waves on the welding impedance value. Unfortunately, the Q55 transducer's amplifier, called Qsonica, is designed to produce vibrations within a specific frequency range. When the transducer is continuously used for a minute, it tends to overheat. Consequently, the output vibrations generated under these overheating conditions are not suitable for ultrasonic-assisted welding applications. Owing to the heating problem, another transducer with a focused horn is used, see Fig. 8 (b-d). Fig. 8 shows the different HPUTs and their positions for producing shear, compressional and contactless vibration at the welding molten pool area during the laser operation.

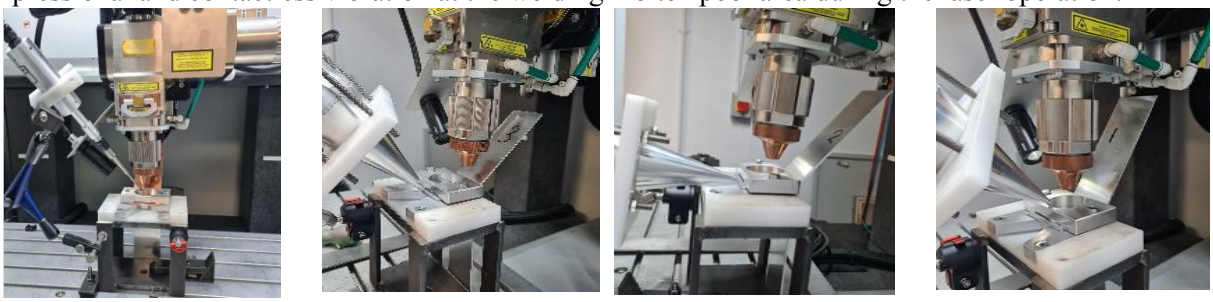

(**a**) (**b**) (**c**) **(d)**

Fig. 8. Ultrasound vibration-assisted welding that involves the use of two types of transducers. Firstly, (a) the Q55 transducer is utilised, and secondly, a transducer with a horn that is compatible with the Brunel Innovation Centre (BIC) amplifier. These transducers are employed to generate different types of vibrations, including (b) contactless, (c) compressional, and (d) shear vibrations.

The HPUT added in this section has a frequency range that closely resembles the Q55 transducer discussed in section 2. As a result, when placed at a similar angle and distance from the plates, it can effectively transmit vibrations to the plates and molten pool area with maximum amplitude. The piezoelectric of the transducer itself might get hot if it is set for continuous operation. To address the potential heating of the piezoelectric component of the transducer during continuous operation, Salimi et al. [29] suggested employing a frequency sweep as a means to indirectly protect the transducer and power generator from potential damage. By utilising a frequency sweep, the operating conditions of the transducer can be varied, preventing excessive heat build-up and safeguarding the integrity of the transducer and power generator. While the vibration level is expected to drop when using contactless vibration compared with contact one [30], it is necessary to find the effect of contact vibration on the welding improvement, in terms of the impedance value. It is important to note that low-intensity ultrasound does not generate any cavitation or shock waves in the molten pool area [31].

For comparison, non-ultrasonic welding was carried out. The average impedance measurement for contactless vibration-assisted welding using the Q55 transducer was determined to be 18 μΩ. In comparison, the results obtained for non-ultrasonic welding yielded an average impedance of 19.1 μΩ. The impedance measurements were repeated by three times averaging to reduce the inclusion of the error. The identical procedure was employed to assess and compare the impact of various wave types on welding quality in terms of impedance value. This involved utilising transducers compatible with the BIC's amplifier to emit shear and compressional waves, as well as contactless excitation. The goal was to determine how each wave type affected the impedance value in welding. The averaged impedance value for the in-plane, out-of-plane, and contactless vibration was found 17 μΩ, 17.8 μΩ and 18 μΩ. The impedance measurements were repeated by three times averaging to reduce the inclusion of the error. A slight improvement in the in-plane excitation is associated with the effective propagation of the compressional wave in both fluid and semifluid medium, while the shear wave can only propagate in the fluid medium.

5. Conclusion

This paper aims to demonstrate the impact of low-intensity ultrasound vibration on improving weld quality of aluminum plates, in terms of impedance value. An industrial HPUT that can be integrated into the laser welding system has been characterised to find the optimum distance and angle from the plate to produce the maximum contactless vibration. The optimum distance to exciting the aluminium plates was found to be 20 mm. The optimal angle for both out-of-plane and in-plane displacement was determined to be 60 degrees. The increased vibration amplification observed at a 60-degree angle may be attributed to the reflection of contactless vibrations from the first plate to the second plate. This reflection leads to a higher overall vibration compared to the configuration at other angles.

The effect of different wave types on laser welding improvement was investigated. While contact vibration leads to an acceleration amplitude approximately 50 times higher than contactless vibration, utilising compressional and shear waves to excite the plate results in improvements of 10% and 6% in the impedance value compared with contactless assisted welding, respectively. Using the contactless ultrasound excitation improved 6 % of the welding quality in terms of the impedance value, compared with the non-ultrasonic sample. The lowest impedance value was associated with ultrasonic-assisted welding with the compressional wave, as the pure fluid cannot support shear wave propagation.

The results and discussions presented in this paper suggest that future work could progress in analysing the weld made in this study in terms of microstructure, grain structure, surface quality, aspect ratio and the tensile test.

6. Reference

[1] Sargent, N.; Jones, M.; Otis, R.; Shapiro, A.A.; Delplanque, J.-P.; Xiong, W. Integration of Processing and Microstructure Models for Non-Equilibrium Solidification in Additive Manufacturing. *Metals (Basel)* **2021**, *11*, 570. https://doi.org/10.3390/met11040570

[2] Yuan, L. Solidification Defects in Additive Manufactured Materials. *Jom* **2019**, *71*, 3221–3222. https://doi.org/10.1007/s11837-019-03662-x

[3] Manvatkar, V.; De, A.; DebRoy, T. Spatial Variation of Melt Pool Geometry, Peak Temperature and Solidification Parameters during Laser Assisted Additive Manufacturing Process. *Materials Science and Technology* **2015**, *31*, 924–930. https://doi.org/10.1179/1743284714Y.0000000701

[4] Sheikhi, M.; Ghaini, F.M.; Assadi, H. Prediction of Solidification Cracking in Pulsed Laser Welding of 2024 Aluminum Alloy. *Acta Mater* **2015**, *82*, 491–502. https://doi.org/10.1016/j.actamat.2014.09.002

[5] Kou, S. A Criterion for Cracking during Solidification. *Acta Mater* **2015**, *88*, 366–374. https://doi.org/10.1016/j.actamat.2015.01.034

[6] Wei, H.L.; Elmer, J.W.; DebRoy, T. Origin of Grain Orientation during Solidification of an Aluminum Alloy. *Acta Mater* **2016**, *115*, 123–131. https://doi.org/10.1016/j.actamat.2016.05.057

[7] Sun, T.; Franciosa, P.; Liu, C.; Pierro, F.; Ceglarek, D. Effect of Micro Solidification Crack on Mechanical Performance of Remote Laser Welded AA6063-T6 Fillet Lap Joint in Automotive Battery Tray Construction. *Applied Sciences* **2021**, *11*, 4522. https://doi.org/10.3390/app11104522

[8] Sun, T.; Franciosa, P.; Sokolov, M.; Ceglarek, D. Challenges and Opportunities in Laser Welding of 6xxx High Strength Aluminium Extrusions in Automotive Battery Tray Construction. *Procedia CIRP* **2020**, *94*, 565–570. https://doi.org/10.1016/j.procir.2020.09.076

[9] Yuan, C.; Deng, Y.; Li, T.; Yang, F. Manufacturing Energy Analysis of Lithium Ion Battery Pack for Electric Vehicles. *CIRP Annals* **2017**, *66*, 53–56. https://doi.org/10.1016/j.cirp.2017.04.109

[10] Hannan, M.A.; Hoque, M.M.; Hussain, A.; Yusof, Y.; Ker, P.J. State-of-the-Art and Energy Management System of Lithium-Ion Batteries in Electric Vehicle Applications: Issues and Recommendations. *Ieee Access* **2018**, *6*, 19362–19378. https://doi.org/10.1109/ACCESS.2018.2817655

[11] Casalino, G. Advances in Welding Metal Alloys, Dissimilar Metals and Additively Manufactured Parts. *Metals (Basel)* 2017, *7*, 32. https://doi.org/10.3390/met7020032

[12] Wang, P.; Chen, X.; Pan, Q.; Madigan, B.; Long, J. Laser Welding Dissimilar Materials of Aluminum to Steel: An Overview. *The International Journal of Advanced Manufacturing Technology* **2016**, *87*, 3081–3090. https://doi.org/10.1007/s00170-016-8725-y

[13] Kolařík, L.; Janovec, J.; Kolaříková, M.; Nachtnebl, P. Influence of Diffusion Welding Time on Homogenous Steel Joints. *Procedia Eng* **2015**, *100*, 1678–1685. https://doi.org/10.1016/j.proeng.2015.01.543

[14] Tathgir, S.; Rathod, D.W.; Batish, A. A-TIG Welding Process for Enhanced-Penetration in Duplex Stainless-Steel: Effect of Activated Fluxes. *Materials and Manufacturing Processes* **2019**, *34*, 1659–1670. https://doi.org/10.1080/10426914.2019.1666990

[15] Kah, P.; Rajan, R.; Martikainen, J.; Suoranta, R. Investigation of Weld Defects in Friction-Stir Welding and Fusion Welding of Aluminium Alloys. *International Journal of Mechanical and Materials Engineering* **2015**, *10*, 1–10. https://doi.org/10.1186/s40712-015-0053-8

[16] Manitsas, D.; Andersson, J. Hot Cracking Mechanisms in Welding Metallurgy: A Review of Theoretical Approaches. In Proceedings of the MATEC Web of Conferences; EDP Sciences, 2018; Vol. 188, p. 03018. https://doi.org/10.1051/matecconf/201818803018

[17] Yin, L.; Zhu, C.; Xu, J.; Zhao, H.; Qiu, J.; Wang, H.; Liu, K. Dynamic Impedance Analysis of Intestinal Anastomosis during High-Frequency Electric Field Welding Process. *Sensors* **2022**, *22*, 4101. https://doi.org/10.3390/s22114101

[18] Wang, Z.; Gao, J.; Bilal, H.M.; Luo, J.; Li, X. Impedance Compensation of the Welding Area of the RF Connector and Microstrip Line. In Proceedings of the 2018 10th International Conference on Communications, Circuits and Systems (ICCCAS); IEEE, 2018; pp. 190–194. https://doi.org/10.1109/ICCCAS.2018.8768967

[19] Sun, Q.J.; Cheng, W.Q.; Liu, Y.B.; Wang, J.F.; Cai, C.W.; Feng, J.C. Microstructure and Mechanical Properties of Ultrasonic Assisted Underwater Wet Welding Joints. *Mater Des* **2016**, *103*, 63–70. https://doi.org/10.1016/j.matdes.2016.04.019

[20] Lei, Z.; Bi, J.; Li, P.; Guo, T.; Zhao, Y.; Zhang, D. Analysis on Welding Characteristics of Ultrasonic Assisted Laser Welding of AZ31B Magnesium Alloy. *Opt Laser Technol* **2018**, *105*, 15–22. https://doi.org/10.1016/j.optlastec.2018.02.050

[21] Liu, J.; Zhu, H.; Li, Z.; Cui, W.; Shi, Y. Effect of Ultrasonic Power on Porosity, Microstructure, Mechanical Properties of the Aluminum Alloy Joint by Ultrasonic Assisted Laser-MIG Hybrid Welding. *Opt Laser Technol* **2019**, *119*, 105619. https://doi.org/10.1016/j.optlastec.2019.105619

[22] Teyeb, A.; Silva, J.; Kanfoud, J.; Carr, P.; Gan, T.-H.; Balachandran, W. Improvements in the Microstructure and Mechanical Properties of Aluminium Alloys Using Ultrasonic-Assisted Laser Welding. *Metals (Basel)* **2022**, *12*, 1041. https://doi.org/10.3390/met12061041

[23] Teyeb, A.; Salimi, M.; El Masri, E.; Balachandran, W.; Gan, T.-H. Analytical Simulation of the Microbubble Collapsing in a Welding Fusion Pool. *Materials* **2023**, *16*, 410. https://doi.org/10.3390/ma16010410

[24] Zuo, Y.Y.; Gong, P.; Ji, S.D.; Li, Q.H.; Ma, Z.W.; Lv, Z. Ultrasound-Assisted Friction Stir Transient Liquid Phase Spot Welded Dissimilar Copper-Aluminum Joint. *J Manuf Process* **2021**, *62*, 58–66. https://doi.org/10.1016/j.jmapro.2020.11.019

[25] Ma, Z.; Jin, Y.; Ji, S.; Meng, X.; Ma, L.; Li, Q. A General Strategy for the Reliable Joining of Al/Ti Dissimilar Alloys via Ultrasonic Assisted Friction Stir Welding. *J Mater Sci Technol* **2019**, *35*, 94–99. https://doi.org/10.1016/j.jmst.2018.09.022

[26] Ahmadnia, M.; Seidanloo, A.; Teimouri, R.; Rostamiyan, Y.; Titrashi, K.G. Determining Influence of Ultrasonic-Assisted Friction Stir Welding Parameters on Mechanical and Tribological Properties of AA6061 Joints. *The International Journal of Advanced Manufacturing Technology* **2015**, *78*, 2009–2024. https://doi.org/10.1007/s00170-015-6784-0

[27] Chen, Q.; Lin, S.; Yang, C.; Fan, C.; Ge, H. Grain Fragmentation in Ultrasonic-Assisted TIG Weld of Pure Aluminum. *Ultrason Sonochem* **2017**, *39*, 403–413. https://doi.org/10.1016/j.ultsonch.2017.05.001

[28] Wolflabs QSONICA - Q55 Available online: https://www.wolflabs.co.uk/laboratory-products/sonicators-probe-type/10335692 (accessed on 20 May 2023).

[29] Salimi, M.; Livadas, M.; Teyeb, A.; El Masri, E.; Gan, T.-H. Biofouling Removal Using a Novel Electronic System for Driving an Array of High Power Marinised Transducers. *Applied Sciences* **2023**, *13*, 3749, doi:10.3390/app13063749. https://doi.org/10.3390/app13063749

[30] Baù, M.; Ferrari, V.; Marioli, D.; Sardini, E.; Serpelloni, M.; Taroni, A. Contactless Excitation and Readout of Passive Sensing Elements Made by Miniaturized Mechanical Resonators. In Proceedings of the SENSORS, 2007 IEEE; IEEE, 2007; pp. 36–39. https://doi.org/10.1109/ICSENS.2007.4388329

[31] Lentacker, I.; De Cock, I.; Deckers, R.; De Smedt, S.C.; Moonen, C.T.W. Understanding Ultrasound Induced Sonoporation: Definitions and Underlying Mechanisms. *Adv Drug Deliv Rev* **2014**, *72*, 49–64. https://doi.org/10.1016/j.addr.2013.11.008